Cheap, versatile, and turnkey fabrication of microfluidic master molds using consumer grade LCD stereolithography 3D printing

Vincent G. Colin[1], Théo A. Travers[1], Denis Gindre[1], Régis Barillé[1], Matthieu Loumaigne[1,*]

[1] *Laboratoire MOLTECH-Anjou, UMR CNRS 6200, UNIV Angers, SFR MATRIX, 2 Bd Lavoisier, 49045 Angers CEDEX, France*

**E-mail: matthieu.loumaigne@univ-angers.fr*

- Section 1 : Direct access to the LCD screen and modification of the gcode.
- Section 2 : Additional practical advices on micro-fabrication with dry film photo resist
- Section 3 : LED spectrum
- Section 4 : Uniformity of the lighting on the LCD screen
- Section 5 : Optical Power Measurement
- Section 6 : Master mold of square pattern
- Section 7 : Imbalance effect in Gradient mixer

1 Direct access to the LCD screen and modification of the gcode.

The information reported here are a priori only relevant for a Phrozen SLA printer.

The firmware files are on a SD card. Since the printer is based on a Raspberry Pi, the system file are in ext3 and are not readable and writable from a Windows computer. We used an Ubuntu virtual machine (using VirtualBox) to access and modify the files on the SD card.

The relevant files are stored in root/python.sla/plates

Two files can be found.

Here is a gcode commented file where only one "plate", that is to say one slice of the 3D object to print, is lighted. The wanted master mold design was on the file "1.png"

```
; Line starting with are comments
```

```
;Filename:Gradient-Mixer
;MachineType:Shuffle_4K
;Volume:0.03168
;Resin:TR-250(LV)
;LayerHeight:0.05
;ResolutinX:2160
;ResolutinY:3840
;MachineX:68.04
;MachineY:120.96
;MachineZ:170.00
;BottomLayerCount:1
;BottomLayerExposureTime:100.0
;NormalExposureTime:100.0
;NormalLiftSpeed:150.0
;NormalDropSpeed:300
;NormalLiftHeight:0.0
;TotalLayers:5

;START_GCODE_BEGIN
G21; Unit conversion metric/imperial
G90; Set Absolute movement
M106 S0; light off
G28 Z0; Ini Axe Z
;START_GCODE_END


;LAYER_START:0
M6054 "1.png"; M6054 show Image
M106 S255; light on
G4 P300000; G4 -> wait 300s
M106 S0; light off
;LAYER_END


;END_GCODE_BEGIN
M106 S0; light off
;G1 Z170.00 F25; Slow Mouvement
M18; Disable stepper.
;END_GCODE_END
```

2 Additional practical advices on micro-fabrication with dryfilm photo resist

Lamination of the dryfilm photoresist.

The dryfilm has to stay protected until the moment it is placed on the smooth substrate (glass microscope slide, PET slide, silicon wafer, etc.) and pressed. The resin used is encased between two thin and transparent protective layers made of Mylan. Waterdrops are deposited on the bare PET substrate in order to facilitate the adhesion of the dryfilm. Then, one of the protective layers is peeled off from the dryfilm, which is placed against the PET substrate without applying any pressure. The water droplets are helping and guiding the adhesion of the dry film through to the other end of the PET substrate. If bubbles or wrinkles appear on the photoresist during this process, a hard rubber roller can be used to smooth them out.

Lamination is performed at a temperature of roughly $100\,°\mathrm{C}$, and a lamination speed of $2\,\mathrm{cm\,s^{-1}}$. If the temperature is not uniform on the roll, as it is apparently the case for consumer-grade ones, an aluminum foil can be placed on top of the protected face of the dryfilm photoresist in order to homogenize the temperature. Lamination at higher temperatures than recommended will create bubbles between the substrate and the dry film photoresist. These bubbles will lead to poor adhesion of the photoresist on the substrate and ultimately to severed microchannels.

Because of the non clean room setting, this step requires a few tries to be mastered, in order to obtain clean samples without creases.

Development of the insolated resin

The development part is accomplished with a K_2CO_3 bath at a concentration of $10\,\mathrm{g\,L^{-1}}$ and at a temperature of of $28°C$. Development at room temperature is also possible but the development time has to be extended.

It is difficult to give a precise development time since it depends on the insolation parameters and the size of the channels on the mold. Nonetheless, one has to examine carefully the insolated film during the whole development process. Indeed, during the first phase of a few minutes, nothing seems to appear on the surface apart from the fact that the bath is progressively tainted in blue. Then, quite quickly, after 15-30 seconds, the blue color of the non-insolated part disappears almost all at once. Then, if the development time is extended for too long (even just a few additional dozens of seconds), the exposed part of the film will also be dissolved. Stated differently, one has to find a compromise between developing sufficiently the non exposed resin and developing for too long causing even the insolated part, in particular the smaller details, to peel off from the substrate.

Development can be stopped at any stage by removing the insolated substrate from the K_2CO_3 bath and rinsing it in clean water. After close inspection with a magnifier or a microscope, the development process can be either stopped or continued by putting back the insolated film in the K_2CO_3 bath.

PDMS curing

To finalize the microchip, the liquid PDMS is poured on the mold to create a negative footprint and then cured for at least for 4 hours at 50-60$°C$. The oven temperature must not exceed this limit. Above this approximative threshold, the dryfilm tends to color in blue the PDMS inside the microchannels.

3 Uniformity of the lighting on the LCD screen

See figure 1.

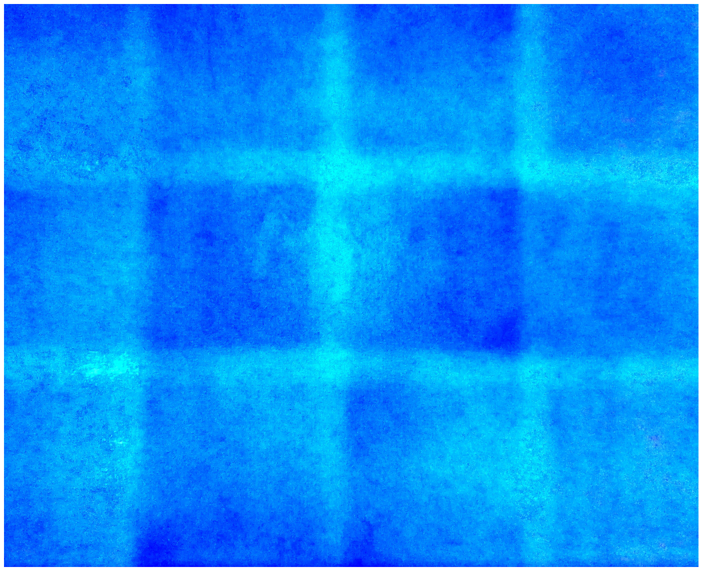

Figure 1 Picture of a paper sheet covering the printer screen with all pixels white. The light emanating from the LED array and the LCD matrix is visualised thanks to the fluorescence of the paper. A grid appears because of the LED array disposition causing a non uniform lighting.

4 Optical power measurement

The luminance of the LED array was estimated using a photodiode (Thorlabs DET100A) with an optical density of 0.5 linked to a 1 MΩ oscilloscope. The photogenerated current was translated to optical power using the constructor data-sheet.

5 Spectrum

The spectrum was measured with a calibrated fibered USB spectrometer (SpectroOvioII) and is shown on fig. 2. The light is emitted from a 405 nm LED. The UV part of the spectra is possibly filtered out by the LCD matrix screen.

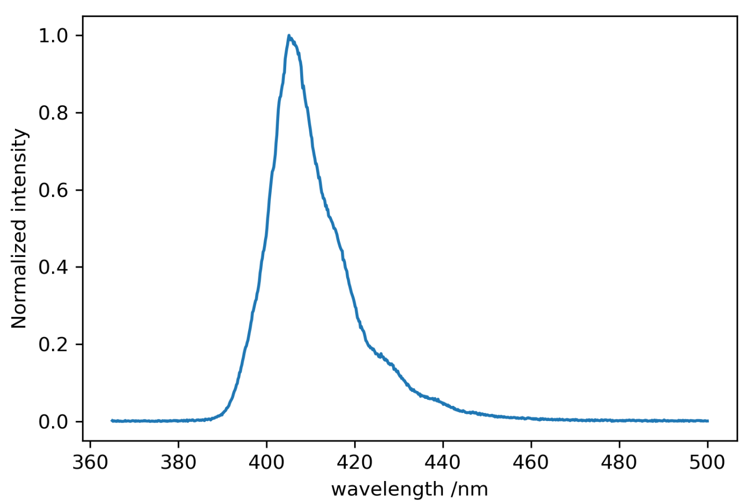

Figure 2 Spectrum of the LED matrix after going trough the LCD panel.

6 Master mold of square pattern

See figure 3 and 4

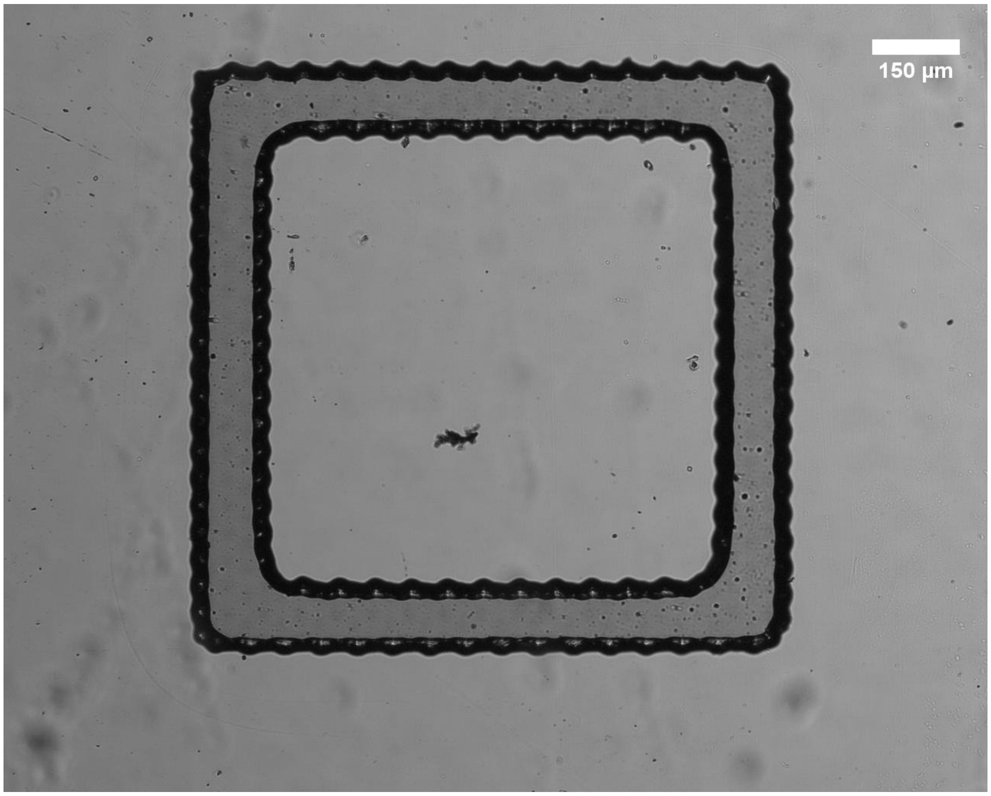

Figure 3 Image of a square pattern insolated with the resin pressed against the LCD matrix. Consequently, sidewall ripples are quite apparent. One can also see the low pass filter effect of the process on the edge of the square.

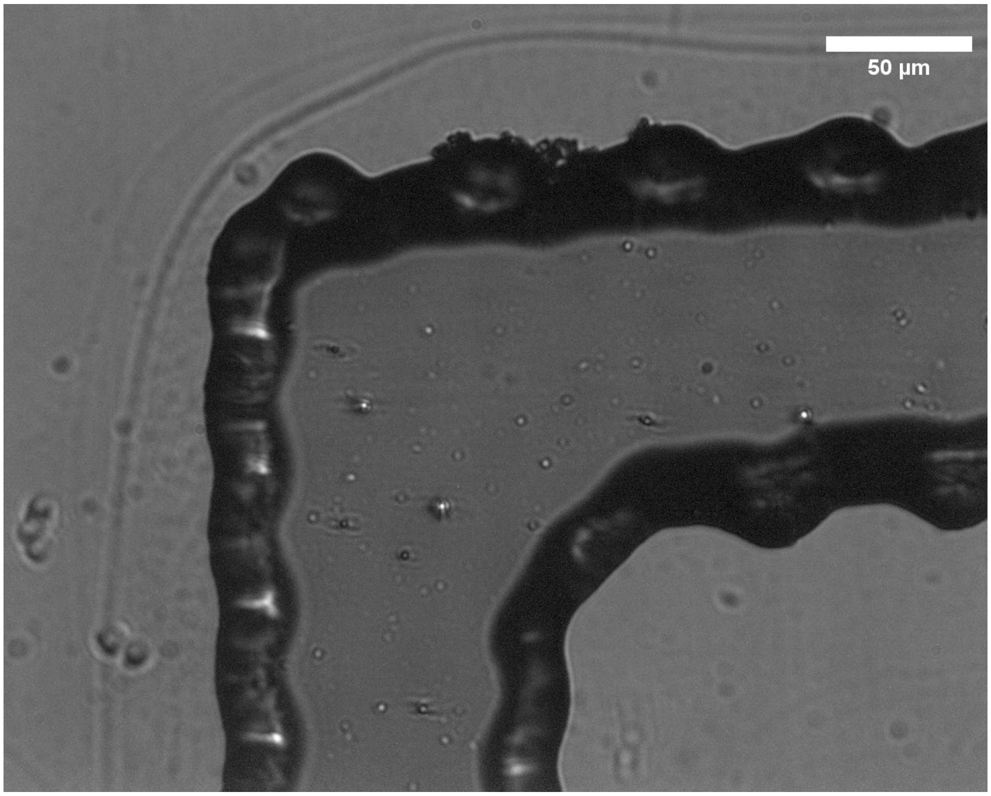

Figure 4 Image of a corner of a square pattern insolated with the resin pressed against the LCD matrix. Consequently, sidewall ripples are quite apparent.

7 Use of a coarser dry film photoresist

See figure 5.

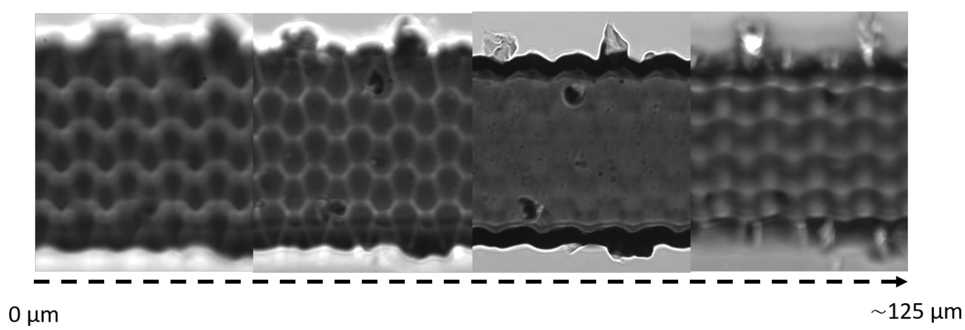

Figure 5 Microscope images at different focalization height of a master mold of a microchannel obtained with a $125\,\mu m$ thick dry film photoresist (Ordyl P50125) pressed against the LCD matrix. One can see what we attribute to the different Fresnel diffraction patterns inscribed inside the resin.

8 Imbalance effect in Gradient mixer

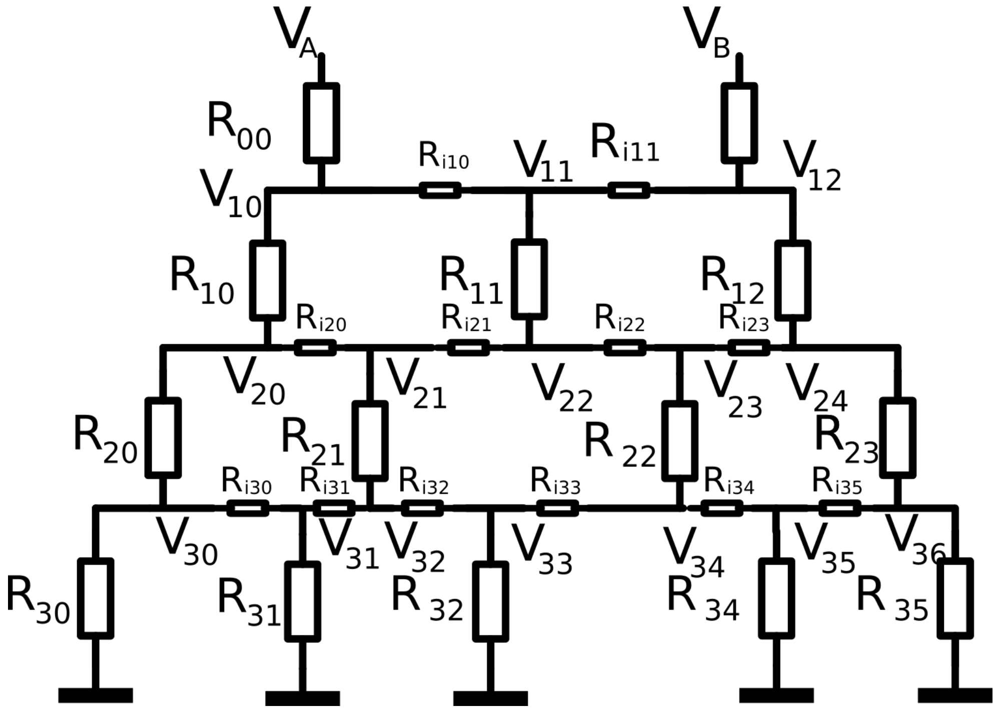

Figure 6 Electric analog of the microfluidics gradient mixer.

We want here to show that a small imbalance in the hydrodynamic resistances of each channel tends to lead the outputs values of the gradient mixer away from the expected theoretical ones.

Following the method proposed by Wang et al. [1], the gradient mixer is modelized by the equivalent circuit shown on figure 6.

Applying Millman theorem on each node of the circuit gives 15 equations that can be rewritten in a matrix form as :

$$YV = A \tag{1}$$

where $V = (V10, V11, V12, V20, V21, V22, V23, V24, V30, V31, V32, V33, V34, V35, V36)$ is the column vector of the searched potentials. Y is a 15x15 matrix translating the 15 equations mentioned above (cf equation 2) and $A = (VA*Y00, 0, VB*Y01, 0, 0, 0, 0, 0, 0, 0, 0, 0, 0, 0, 0)$, where $Yij = 1/Rij$ and V_A and V_B are the input potential.

The equation 1 is solved numerically in order to obtain the different potential/pressure at each node. Currents (i.e. flow) are obtained using Ohm's law.

The evolution of the concentration profile along the channels, the splitters and the combiners is represented in terms of Fourier series[1].

Beginning with a perfectly balanced network, each hydrodynamic resistance is multiplied by $(1+\sigma)$ where σ is a gaussian distributed random variable so that the relative error has the standard deviation σ. For each value of sigma, 500 different random networks are generated and their outputs is computed. Then, the mean value and the standard deviation for the 500 experiment are calculated for each output. Figure 7 presents the evolution of this standard deviation normalised by the mean value of each output for different value of the random modification of the hydrodynamic radius with standard deviation σ.

For instance, we can see that a random error with a standard deviation σ of 10% on hydrodynamic radius affect dramatically the output number 3, whose theoretical output value is $c/4$. Although the mean output value computed with 500 different random network is still close from c/4, the standard deviation is around 30% meaning that a lot of gradient mixer chip doesn't work has intended.

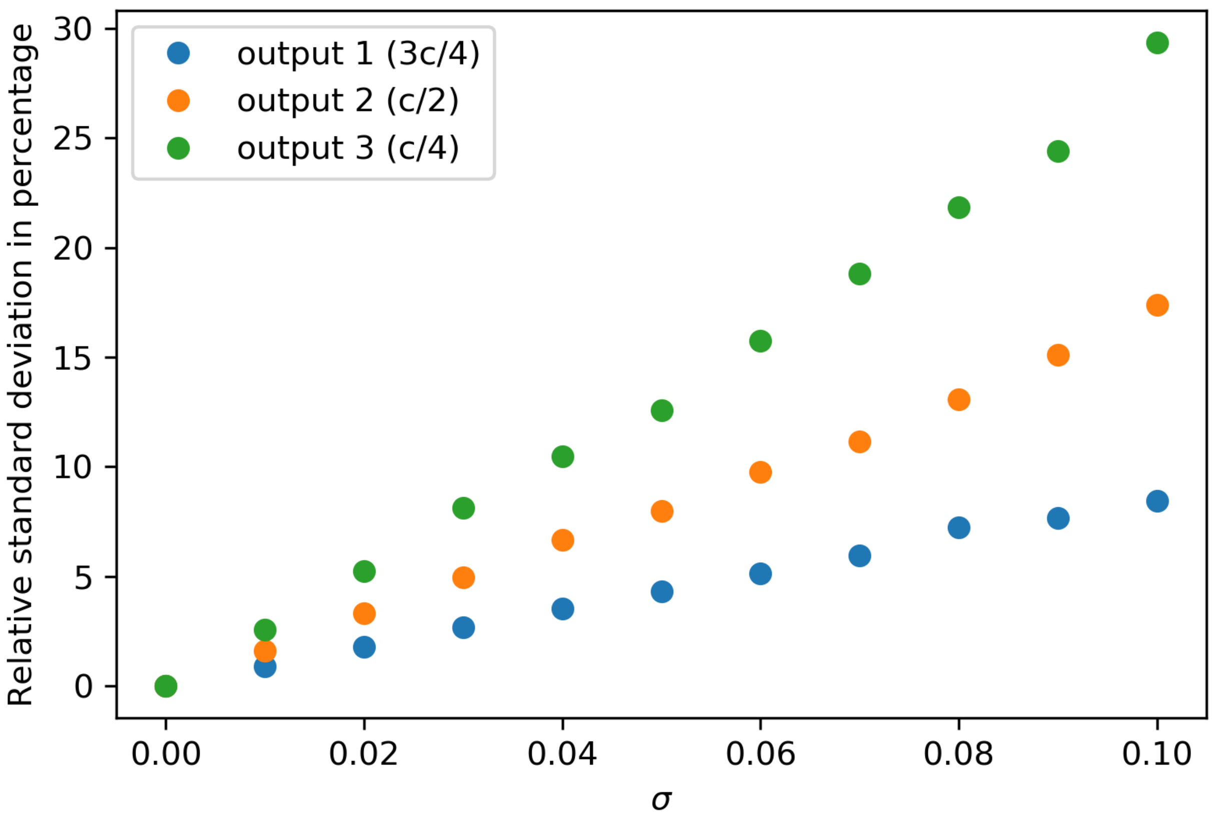

Figure 7 Evolution of the relative standard error (standard deviation/mean) for different value standard deviation σ of the random error on hydrodynamic radius among the network.

The corresponding python code can be found at `https://github.com/MLoum/ImbalanceGradientMixer`

 NOTES AND REFERENCES

$$
Y = \begin{bmatrix}
Y10+Y00+Yi10 & -Yi10 & 0 & -Y10 & 0 & 0 & 0 & 0 & 0 & 0 \\
0 & 0 & 0 & 0 & 0 & & & & & \\
-Yi10 & Y11+Yi10+Yi11 & -Yi11 & 0 & 0 & -Y11 & 0 & 0 & 0 & 0 \\
0 & 0 & 0 & 0 & 0 & & & & & \\
0 & -Yi11 & Y12+Y01+Yi11 & 0 & 0 & 0 & 0 & -Y12 & 0 & 0 \\
0 & 0 & 0 & 0 & 0 & & & & & \\
-Y10 & 0 & 0 & Y20+Y10+Yi20 & -Yi20 & 0 & 0 & 0 & -Y20 & 0 \\
0 & 0 & 0 & 0 & 0 & & & & & \\
0 & 0 & 0 & -Yi20 & Yi20+Yi21+Y21 & -Yi21 & 0 & 0 & 0 & 0 \\
-Y21 & 0 & 0 & 0 & 0 & & & & & \\
0 & -Y11 & 0 & 0 & -Yi21 & Yi21+Yi22+Y11 & -Yi22 & 0 & 0 & 0 \\
0 & 0 & 0 & 0 & 0 & & & & & \\
0 & 0 & 0 & 0 & 0 & -Yi22 & Yi22+Yi23+Y22 & -Yi23 & 0 & 0 \\
0 & 0 & -Y22 & 0 & 0 & & & & & \\
0 & 0 & -Y12 & 0 & 0 & 0 & -Yi23 & Yi23+Y12+Y23 & 0 & 0 \\
0 & 0 & 0 & 0 & -Y23 & & & & & \\
0 & 0 & 0 & -Y20 & 0 & 0 & 0 & 0 & Y30+Y20+Yi30 & -Yi30 \\
0 & 0 & 0 & 0 & 0 & & & & & \\
0 & 0 & 0 & 0 & 0 & 0 & 0 & 0 & -Yi30 & Yi30+Y31+Yi31 \\
-Yi31 & 0 & 0 & 0 & 0 & & & & & \\
0 & 0 & 0 & 0 & -Y21 & 0 & 0 & 0 & 0 & -Yi31 \\
Yi31+Y21+Yi32 & -Yi32 & 0 & 0 & 0 & & & & & \\
0 & 0 & 0 & 0 & 0 & 0 & 0 & 0 & 0 & 0 \\
-Yi32 & Yi32+Y32+Yi33 & -Yi33 & 0 & 0 & & & & & \\
0 & 0 & 0 & 0 & 0 & -Y22 & 0 & 0 & 0 & 0 \\
0 & -Yi33 & Yi33+Y22+Yi34 & -Yi34 & 0 & & & & & \\
0 & 0 & 0 & 0 & 0 & 0 & 0 & 0 & 0 & 0 \\
0 & 0 & -Yi34 & Yi34+Y33+Yi35 & -Yi35 & & & & & \\
0 & 0 & 0 & 0 & 0 & 0 & -Y23 & 0 & 0 & 0 \\
0 & 0 & 0 & -Yi35 & Yi35+Y23+Y34 & & & & &
\end{bmatrix} \tag{2}
$$

Notes and references

[1] Systematic modeling of microfluidic concentration gradient generators. *Journal of Micromechanics*

and Microengineering, 16(10):2128–2137, 2006.